Title	Influence of localized surface plasmon resonance and free electrons on the optical properties of ultrathin Au films : a study of the aggregation effect
Author(s)	Li, X. D.; Chen, T. P.; Liu, Y.; Leong, K. C.
Citation	Li, X. D., Chen, T. P., Liu, Y., & Leong, K. C. (2014). Influence of localized surface plasmon resonance and free electrons on the optical properties of ultrathin Au films: a study of the aggregation effect. Optics Express, 22(5), 5124-5132.
Date	2014
URL	http://hdl.handle.net/10220/19068
Rights	© 2014 Optical Society of America. This paper was published in Optics Express and is made available as an electronic reprint (preprint) with permission of Optical Society of America. The paper can be found at the following official DOI: [http://dx.doi.org/10.1364/OE.22.005124]. One print or electronic copy may be made for personal use only. Systematic or multiple reproduction, distribution to multiple locations via electronic or other means, duplication of any material in this paper for a fee or for commercial purposes, or modification of the content of the paper is prohibited and is subject to penalties under law.

Influence of localized surface plasmon resonance and free electrons on the optical properties of ultrathin Au films: a study of the aggregation effect

X. D. Li,[1,*] T. P. Chen,[1,4] Y. Liu,[2] and K. C. Leong[3]

[1]*School of Electrical and Electronic Engineering, Nanyang Technological University, 639798 Singapore*
[2]*State Key Laboratory of Electronic Thin Films and Integrated Devices, University of Electronic Science and Technology, Chengdu 610054, China*
[3]*GLOBALFOUNDRIES Singapore Pte Ltd, 738406 Singapore*
[4]*echentp@ntu.edu.sg*
[*]*lixi0042@e.ntu.edu.sg*

Abstract: The contributions of localized surface plasmon resonance (LSPR) and Drude (free electrons) absorption to the complex dielectric function of ultrathin Au films were investigated with spectroscopic ellipsometry. When the Au film thickness is thinner than ~10 nm, Au nanoparticles (NPs) are formed as a result of the discontinuity in the films, leading to the emergence of LSPR of Au NPs; and the LSPR exhibits a splitting when the films thinner than ~8 nm, which could be attributed to the near-field coupling of the Au NPs and/or the inhomogeneous polarizations of the Au NPs. On the other hand, the delocalization of electrons in Au NPs due to the aggregation of Au NPs in a thicker film leads to an increase in the free-electron absorption and a suppression of the LSPR.

OCIS codes: (160.3900) Metals; (160.4236) Nanomaterials; (260.2130) Ellipsometry and polarimetry; (240.6680) Surface plasmons; (120.4530) Optical constants.

References and links

1. L. J. Sherry, S.-H. Chang, G. C. Schatz, R. P. Van Duyne, B. J. Wiley, and Y. Xia, "Localized surface plasmon resonance spectroscopy of single silver nanocubes," Nano Lett. **5**(10), 2034–2038 (2005).
2. K. A. Willets and R. P. Van Duyne, "Localized surface plasmon resonance spectroscopy and sensing," Annu. Rev. Phys. Chem. **58**(1), 267–297 (2007).
3. T. R. Jensen, M. D. Malinsky, C. L. Haynes, and R. P. Van Duyne, "Nanosphere lithography: tunable localized surface plasmon resonance spectra of silver nanoparticles," J. Phys. Chem. B **104**(45), 10549–10556 (2000).
4. Y. Yang, S. Matsubara, M. Nogami, J. Shi, and W. Huang, "One-dimensional self-assembly of gold nanoparticles for tunable surface plasmon resonance properties," Nanotechnology **17**(11), 2821–2827 (2006).
5. X. Li, L. Jiang, Q. Zhan, J. Qian, and S. He, "Localized surface plasmon resonance (LSPR) of polyelectrolyte-functionalized gold-nanoparticles for bio-sensing," Colloid Surf. A Physicochem. Eng. Aspects **332**(2-3), 172–179 (2009).
6. U. Kreibig and M. Vollmer, *Optical Properties of Metal Clusters* (Springer, 1995), Chap. 2.
7. P. Clippe, R. Evrard, and A. A. Lucas, "Aggregation effect on the infrared absorption spectrum of small ionic crystals," Phys. Rev. B **14**(4), 1715–1721 (1976).
8. S. Link and M. A. El-Sayed, "Optical properties and ultrafast dynamics of metallic nanocrystals," Annu. Rev. Phys. Chem. **54**(1), 331–366 (2003).
9. R. G. Barrera, M. Del Castillo Mussot, G. Monsivais, P. Villaseor, and W. L. Mochán, "Optical properties of two-dimensional disordered systems on a substrate," Phys. Rev. B Condens. Matter **43**(17), 13819–13826 (1991).
10. H. Wormeester, A.-I. Henry, E. S. Kooij, B. Poelsema, and M.-P. Pileni, "Ellipsometric identification of collective optical properties of silver nanocrystal arrays," J. Chem. Phys. **124**(20), 204713 (2006).
11. T. Atay, J.-H. Song, and A. V. Nurmikko, "Strongly interacting plasmon nanoparticle pairs: from dipole–dipole interaction to conductively coupled regime," Nano Lett. **4**(9), 1627–1631 (2004).

#203279 - $15.00 USD Received 17 Dec 2013; revised 18 Feb 2014; accepted 18 Feb 2014; published 26 Feb 2014

12. J. C. M. Garnett, "Colours in metal glasses and in metallic films," Philos. Trans. R. Soc. London **203**(359-371), 385–420 (1904).
13. D. A. G. Bruggeman, "Calculation of various physical constants of heterogeneous substances. I. dielectric constant and conductivity of mixtures of isotropic substances," Ann. Phys. **24**, 636–664 (1935).
14. R. W. Cohen, G. D. Cody, M. D. Coutts, and B. Abeles, "Optical properties of granular silver and gold films," Phys. Rev. B **8**(8), 3689–3701 (1973).
15. A. Meessen, "The anomalous infra-red absorption of alkali metals and collective oscillations in small metal particles," J. Phys. **33**(4), 371–381 (1972).
16. A. D. Rakic, A. B. Djurisic, J. M. Elazar, and M. L. Majewski, "Optical properties of metallic films for vertical-cavity optoelectronic devices," Appl. Opt. **37**(22), 5271–5283 (1998).
17. P. Romaniello and P. L. de Boeij, "The role of relativity in the optical response of gold within the time-dependent current-density-functional theory," J. Chem. Phys. **122**(16), 164303 (2005).
18. R. Lässer and N. V. Smith, "Interband optical transitions in gold in the photon energy range 2–25 eV," Solid State Commun. **37**(6), 507–509 (1981).
19. E. D. Palik and G. Ghosh, *Handbook of Optical Constants of Solids* (Academic, 1998).
20. R. M. A. Azzam and N. M. Bashara, *Ellipsometry and Polarized Light* (North-Holland, 1977), Chap. 3.
21. P. Nordlander, C. Oubre, E. Prodan, K. Li, and M. I. Stockman, "Plasmon hybridization in nanoparticle dimers," Nano Lett. **4**(5), 899–903 (2004).
22. H. Wang, D. W. Brandl, P. Nordlander, and N. J. Halas, "Plasmonic nanostructures: artificial molecules," Acc. Chem. Res. **40**(1), 53–62 (2007).
23. T. W. H. Oates and A. Mücklich, "Evolution of plasmon resonances during plasma deposition of silver nanoparticles," Nanotechnology **16**(11), 2606–2611 (2005).
24. A. Hilger, M. Tenfelde, and U. Kreibig, "Silver nanoparticles deposited on dielectric surfaces," Appl. Phys. B **73**(4), 361–372 (2001).

1. Introduction

Metallic nanoparticles such as gold and silver nanoparticles exhibit remarkable visible-absorption peak which is absent in their bulk counterpart. This characteristic absorption peak is related to the collective oscillation of conduction electrons inside the nanoparticles, known as localized surface plasmon resonance (LSPR). LSPR is strongly dependent of the nanoparticle size, shape, inter-particle spacing and surrounding medium [1, 2]. By tuning these parameters, the LSPR can be used for important sensing and spectroscopy applications [3–5]. It has been shown that structural geometry of individual particles and the aggregate topology have significantly impact on the optical response of nanoparticles, in particular, the surface plasmon resonance [6, 7]. As the discrete nanoparticles aggregate, the effect of higher multipoles resulted from the irregular particle shapes and dipole-dipole interactions between the nearest particles could greatly modify the LSPR of the nanoparticles system, e.g., red-shift of LSPR due to the inhomogeneous polarization of nanoparticles [8, 9], and splitting of LSPR due to the near-field coupling between neighboring nanoparticles [10, 11]. On the other hand, unlike discrete nanoparticles where the resonances of the electrons dominant in the optical absorption, aggregated nanoparticles exhibit non-negligible Drude (free electrons) absorption as a result of the formation of percolation paths between the neighboring nanoparticles, which could greatly delocalize the free electrons inside the nanoparticles and lead to the suppression of plasmon resonance. Therefore, it is interesting to study the contributions of LSPR and Drude absorption to the optical response of an aggregated nanoparticle system, and knowing the evolution of dielectric function of an ultrathin metal film with aggregation of the metal nanoparticles is definitely important for various applications.

In this work, a systematic study of aggregation effect on the dielectric function of ultrathin Au films consisting of self-assembled gold nanoparticles (Au NPs) on SiO_2 is conducted. The Au thin films were deposited on quartz or silicon substrate covered with a thin SiO_2 layer using electron-beam (e-beam) evaporation technique. It has been observed that Au NPs aggregate into large-scale coalescence with increasing film thickness, and inter-links between the particles are gradually formed. A continuous film is observed with the film thickness of 10 nm; and discontinuous Au NP thin films are formed for the films thinner than ~10 nm. The dielectric function of self-assembled gold nanoparticles on SiO_2 has been determined with spectroscopic ellipsometry (SE) based on the Drude and Lorentz dispersion functions. Size

#203279 - $15.00 USD Received 17 Dec 2013; revised 18 Feb 2014; accepted 18 Feb 2014; published 26 Feb 2014

dependence of the optical properties (refractive index n and distinction coefficient k) of Au NPs has been studied. The result shows that the aggregation effect has a significant influence on the LSPR and Drude absorption of the Au NP films.

2. Experiment

A *p*-type silicon wafer was first cleaned by diluted HF solution to remove the native oxide. Subsequently, a 30 nm SiO_2 buffer layer was grown on the silicon substrate by dry oxidation. Au films with nominal thicknesses of 4, 5, 6, 8, 10 nm were deposited on the SiO_2 layer or a quartz substrate by electron beam evaporation in the pressure of 4×10^{-6} mbar. The deposition rate was maintained at 0.1 Å per second. The oxide buffer layer was used to prevent the silicidation reaction between the deposited Au films and the Si substrate and provide a film structure configuration (Au NP film / SiO_2 layer) that is similar to the one (Au NP film /quartz substrate) used in the optical absorbance measurement. The film surface morphology was investigated using high resolution scanning electron microscope (HRSEM) (LEO 1550 Gemini). Optical absorbance measurement was carried out with an UV-Vis spectrophotometer (Perkin-Elmer 950) on the samples of Au NP films deposited on quartz substrate in the wavelength range of 250-2500 nm. The quartz substrate is used as the reference baseline for all the absorbance measurement. Complex dielectric function of the Au NPs was obtained with spectroscopic ellipsometry (SE) (Woollam VB-250) on the samples of Au NP films deposited on the SiO_2 layer in the wavelength range of 250-1200 nm.

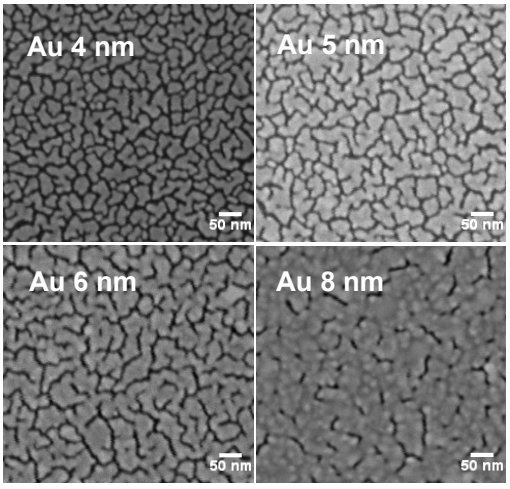

Fig. 1. HRSEM images of the ultrathin Au films with the nominal thicknesses of 4-8 nm on the SiO_2 layer.

Figure 1 shows the HRSEM images of the Au NP films with the film thicknesses of 4, 5, 6 and 8 nm, respectively. As shown in the figure, the Au films with the thicknesses of 4, 5 and 6 nm exhibit a large-scale coalescence of Au NPs and a high surface coverage on SiO_2. The average size and irregularity of the Au NPs increase with increasing film thickness. The formation of worm-like particles is the direct evidence of aggregation of Au NPs on the SiO_2 layer due to touching and merging of adjacent particles. The formation of inter-links between the coalescences of Au NPs is greatly enhanced as the film continues growing, and a continuous film is eventually formed as the film thickness reaches ~10 nm.

3. Absorbance measurement

Figure 2 shows the absorbance spectra of the ultrathin Au films with various thicknesses on quartz substrate in the photon energy range of 0.5-5 eV at room temperature. The influence of

#203279 - $15.00 USD Received 17 Dec 2013; revised 18 Feb 2014; accepted 18 Feb 2014; published 26 Feb 2014

the film thickness on the absorbance spectrum is evident in the figure. A difference in the film thickness means a difference in the degree of aggregation, which can be translated to the differences in the particle size, shape and interparticle distance. Unlike the bulk Au where the Drude absorption (free-electrons) dominates in the infrared, metal nanoparticle film exhibits LSPR in the visible region [6]. As shown in Fig. 2, the aggregation effect is obvious in the region with photon energies lower than ~2.5 eV where the Drude absorption and the LSPR occur. As the film thickness decreases, the Drude absorption is reduced, while the LSPR is enhanced. A LSPR band can be observed for the films thinner than 8 nm. The enhancement of the plasmon resonance is associated with the reduction of Drude absorption as a result of the decrease of aggregation of Au NPs in a thinner film. In a thicker film, the formation of inter-links (conductive percolation paths) between the Au NPs due to the aggregation of Au NPs can delocalize the free electrons inside the particles, the concentration of free electrons is higher, and thus the Drude absorption is more significant. However, the aggregation will suppress the LSPR of the Au NPs. On the other hand, a red-shift of the LSPR with increasing film thickness is observed. The phenomenon can be attributed to the inhomogeneous polarization of the nanoparticles with larger sizes, which enhances the higher-order-mode oscillations at lower energies [8]. Note that the red shift of LSPR of the 6 nm film relative to the 5 nm film is difficult to observe in Fig. 2 due to the overlap of the Drude absorption and the LSPR band as result of the significant aggregation of Au NPs in a thicker film (> 4 nm) (however, it could be revealed by a curve fitting program).

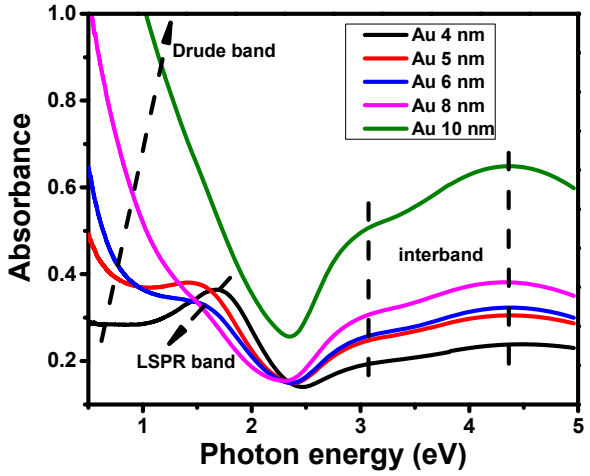

Fig. 2. Absorbance spectra of the ultrathin Au films with various thicknesses on quartz substrate.

4. Ellipsometric modeling

To quantitatively understand the contributions of the LSPR and Drude band to the optical response of the aggregated nanoparticles film, the complex dielectric function of the aggregated Au NPs were determined with the spectroscopic ellipsometry (SE). The ellipsometric angles (Ψ and Δ) were measured on the samples of Au NP thin films on the SiO_2 layer in the wavelength range of 250-1200 nm with a step size of 5 nm at an incident angle of 75°. The Au NP thin film system can be treated as a quasi-homogeneous effective-medium material, which can be described with an effective medium approximation (EMA). Maxwell-Garnett (MG) EMA [12] and Bruggeman EMA [13] are the common approaches to describe the dielectric properties of particles embedded in a dielectric host matrix. However, both MG and Bruggeman EMAs are valid only for a low particle volume fraction and fail to describe particle-particle interactions in the scenario of a high volume fraction. Cohen *et al* [14] has proposed a generalized EMA, which has the form [14]

#203279 - $15.00 USD Received 17 Dec 2013; revised 18 Feb 2014; accepted 18 Feb 2014; published 26 Feb 2014

$$\frac{\varepsilon_e - \varepsilon_m}{(\varepsilon_e - \varepsilon_m)L_i + \varepsilon_m} = (1-Q)\frac{\varepsilon_i - \varepsilon_m}{(\varepsilon_i - \varepsilon_m)L_i + \varepsilon_m}. \quad (1)$$

where ε_e is the effective complex dielectric function of the Au NP film, ε_m is the complex dielectric function of Au NPs, ε_i is the complex dielectric function of the surrounding dielectric material (here it is air), and L_i is the effective depolarization factor of the surrounding dielectric material, Q is the filling factor of Au NPs. The effective depolarization factor L_i here can be interpreted as the quantity that describes the lateral interactions in the Au NP/dielectric system [14, 15].

In the dielectric function of the aggregated Au NPs, the free electrons absorption can be described by the Drude dispersion function, and both the LSPR peaks and interband transitions can be represented with a Lorentz dispersion function, as given below [16]

$$\varepsilon_m(E) = (1 - \frac{f_0 E_p^2}{E^2 + i\Gamma_0 E}) + \sum_{j=1}^{k} \frac{f_j E_p^2}{E_j^2 - E^2 - i\Gamma_j E}. \quad (2)$$

where (f_0 , Γ_0) and (f_j , Γ_j) are (oscillator strength, broadening parameter) for the Drude and Lorentz dispersion functions, respectively. E_p is the plasma energy, E_j is the resonance energy. As shown in Fig. 2, there are two broaden absorption peak observed at ~3.05 eV and ~4.32 eV, which can be attributed to the interband transitions from *d*-valance band to the empty states in the *s* and *p* bands above the Fermi level [17, 18]. It is observed in the figure that the interband transitions are not largely affected by the structural properties of the nanoparticles. In order to simplify the optimization process during the SE spectral fitting, the two interband transitions of the aggregated Au NPs are modeled with two Lorentz dispersion functions with the resonance energies fixed at 3.05 and 4.32 eV, respectively.

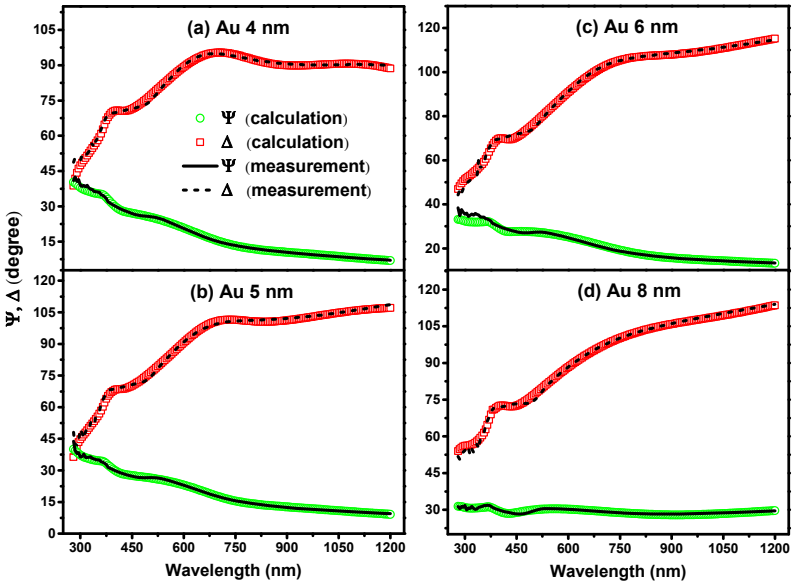

Fig. 3. SE spectral fittings of the Au NP films with the film thicknesses of 4-8 nm on the SiO_2 layer that is thermally grown on a silicon substrate. The ellipsometric angles Ψ and Δ are measured at the incident angle of 75°.

#203279 - $15.00 USD Received 17 Dec 2013; revised 18 Feb 2014; accepted 18 Feb 2014; published 26 Feb 2014

Figure 3 shows the SE spectral fittings of the measured ellipsometric angles (Ψ, Δ) for the Au NP films with the film thicknesses of 4-8 nm using Eqs. (1) and (2) and based on the four-phase model (i.e., air/Au NP film/SiO_2/Si). In the calculation of Ψ and Δ, the complex dielectric functions of SiO_2 and bulk Si from [19] were used. The effective dielectric function of the Au NP films is calculated with Eq. (1) under the assumption that air void ($\varepsilon_i = 1$) is embedded in the Au NP films with the Au NPs as the host material. The filling factor (Q) of the Au NPs in the Au NP films on SiO_2 estimated from the SEM images are ~76%, 83%, 85%, and 90% for the Au NP films with the film thicknesses of 4, 5, 6, and 8 nm, respectively. The measured ellipsometric data (Ψ, Δ) were fitted in the wavelength range of 280-1200 nm by minimizing the mean-squared-error of the difference between the calculated and experimentally measured Ψ and Δ [20]. As shown in Fig. 3, the calculated Ψ and Δ yielded from the best spectral fittings show good agreement with the measured data (Ψ and Δ) in the wavelength range of 400-1200 nm. Figures 4(a) and 4(b) show the real ($\varepsilon_{m,1}$) and imaginary ($\varepsilon_{m,2}$) parts of the complex dielectric function of the Au NPs of the Au NP films with various film thicknesses yielded from the SE spectral fittings, respectively. The real ($\varepsilon_{e,1}$) and imaginary ($\varepsilon_{e,2}$) parts of the effective complex dielectric function calculated with Eq. (1) for the Au NP films with the film thicknesses of 4-8 nm are shown in Figs. 4(c) and 4(d), respectively.

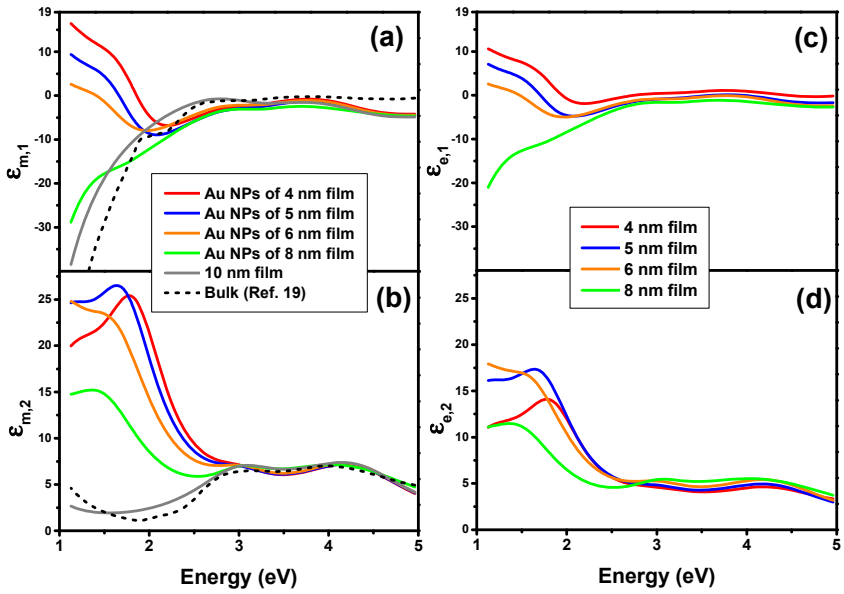

Fig. 4. (a) Real part ($\varepsilon_{m,1}$) and (b) imaginary part ($\varepsilon_{m,2}$) of the complex dielectric function of the Au NPs of the Au NP films with the film thicknesses of 4-8 nm. The complex dielectric functions of the continuous Au film with the thickness of 10 nm and the bulk Au (Ref. 19) are included in the two figures for comparison. (c) The real part ($\varepsilon_{e,1}$) and (d) imaginary part ($\varepsilon_{e,2}$) of the effective complex dielectric function of the Au NP films with the film thicknesses of 4-8 nm.

#203279 - $15.00 USD Received 17 Dec 2013; revised 18 Feb 2014; accepted 18 Feb 2014; published 26 Feb 2014

5. Discussions

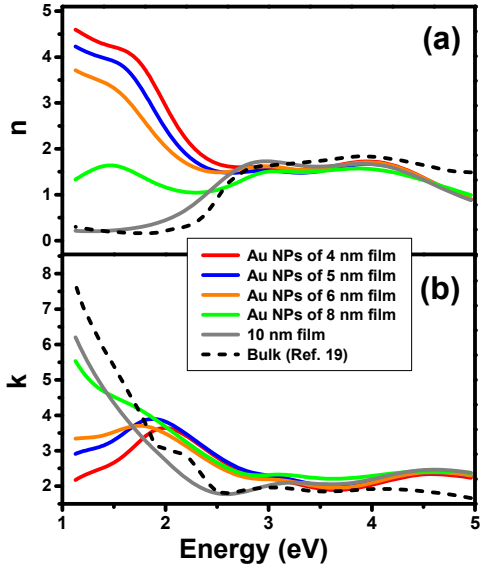

Fig. 5. (a) Refraction index n and (b) extinction coefficient k of the Au NPs of the Au NP films with film thicknesses of 4-8 nm. The optical constants of both the continuous Au film with thickness of 10 nm and the bulk Au (Ref. 19) are included for comparison.

Figures 5(a) and 5(b) show the refraction index (n) and extinction coefficient (k) of the Au NPs of the Au NP films, which are obtained from the calculation using the complex dielectric function of the Au NPs shown in Figs. 4(a) and 4(b). The optical constants of the continuous Au film with the thickness of 10 nm and the bulk Au are also included in Fig. 5 for comparison. It can be observed from the figure that the optical constants (n, k) of the Au NPs become more similar to that of bulk Au as the film thickness increases, as a result of aggregation of the Au NPs into large-scale of coalescence, which eventually leads to a continuous film. As shown in Fig. 5(b), the Au NP films with the film thicknesses of 4, 5 and 6 nm exhibit a broaden absorption peak in the energy range of 1-2.5 eV due to the collective oscillation of the conduction electrons inside the Au NPs. The broadening of LSPR can be attributed to the splitting of plasmon resonance, which was modeled with two Lorentz oscillators (SPR1 and SPR2) in the SE analysis. The resonance energies of SPR1 and SPR2 as a function of the film thickness are shown in Fig. 6. It has been shown that the near-field coupling of the nanoparticle pairs could cause the splitting of plasmon band as a result of excitation of multipole mode in non-spherical particles [11]. The origin of the splitting could be attributed to the hybridization of plasmon of the individual nanoparticles, and the strength of the hybridization strongly depends on the geometry of the composite particles [21, 22]. The splitting of plasmon band could also be attributed to the inhomogeneous polarizations of nanoparticles [23, 24], which typically result in a red-shift of plasmon resonance. As shown in Fig. 6, both the SPR1 and SPR2 show a red-shift with increasing film thickness. In a classic description, the red shift of plasmon band indicates a reduction of oscillation of electrons due to the reduction of restoring force as a result of inhomogeneous polarizations in a particle with large size and irregular shape. Therefore, the LSPR could be greatly influenced by the aggregation topology of the nanoparticles. On the other hand, the formation of percolation paths in a thicker film leads to an increase of the Drude (free electrons) absorption, which could overlap with the LSPR band and result in an increase of absorption at low energies. This argument is supported by the results shown in Fig. 5(b). For the Au film with thickness of 10 nm, the LSPR band disappears and is superseded by the Drude

#203279 - $15.00 USD Received 17 Dec 2013; revised 18 Feb 2014; accepted 18 Feb 2014; published 26 Feb 2014

absorption. This indicates a complete transition from an aggregated Au NP film to an electrically continuous Au film. Therefore, the dielectric function of the continuous Au film with thickness of 10 nm is close to that of bulk Au, as shown in Fig. 4.

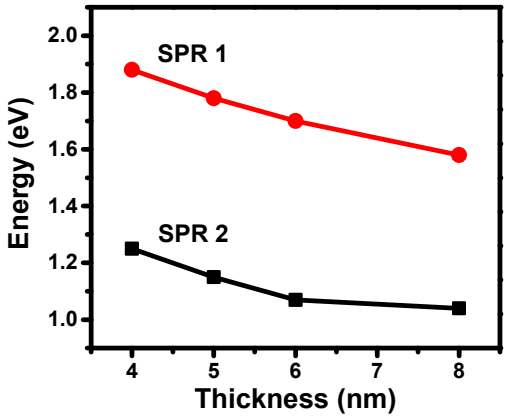

Fig. 6. Red-shifts of the resonance energies of SPR 1 and SPR 2 with the thickness of the Au NP films.

Figures 7(a) and 7(b) show the contributions of the Drude band (k_{Drude}) and LSPR band (k_{LSPR}) to the extinction coefficient (k) of the Au NPs of the Au NP films with different thicknesses, respectively. As discussed earlier, the aggregation of the Au NPs has significant impact on the particle size, shape and interparticle distance, which directly influence the optical response of the Au NP film. As shown in Fig. 7(a), the Drude absorption increases with increasing film thickness. This is a direct evidence of the increase of free electrons concentration in a thicker film due to the delocalization of electrons in the aggregated Au NPs. The aggregation of nanoparticles is more significant in a thicker film. On the other hand, the delocalization of electrons suppresses the LSPR in a thicker film, which is indeed observed in Fig. 7(b).

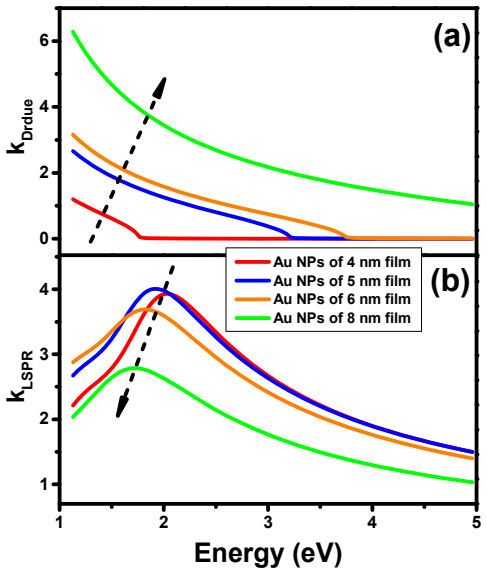

Fig. 7. Contributions of the Drude band (a) and LSPR band (b) to the extinction coefficient k of the Au NPs of the Au NP films with film thicknesses of 4-8 nm.

#203279 - $15.00 USD Received 17 Dec 2013; revised 18 Feb 2014; accepted 18 Feb 2014; published 26 Feb 2014

6. Conclusion

Aggregation effect on the LSPR and Drude absorption of Au NPs of Au NP films with various film thicknesses has been investigated with SE. The splitting of the plasmon resonance is observed for the ultrathin films thinner than ~8 nm, which could be attributed to the near-field coupling of the Au NPs and/or the inhomogeneous polarizations of the nanoparticles. In a thicker film, the aggregation of the Au NPs leads to the delocalization of electrons in the Au NPs, causing an increase in the free-electron concentration and thus an increase in the Drude absorption; however, the delocalization reduces the LSPR band.

Acknowledgments

This work is financially supported by MOE Tier 1 Grant (Grant No. RG 43/12) and A*Star-NTU Si COE Program. Y. Liu would like to acknowledge the support by NSFC under Project No. 61274086.

#203279 - $15.00 USD Received 17 Dec 2013; revised 18 Feb 2014; accepted 18 Feb 2014; published 26 Feb 2014